Nanoscale Res Lett (2009) 4:452–458
DOI 10.1007/s11671-009-9269-y

NANO EXPRESS

Nanometer Sized Silver Particles Embedded Silica Particles—Spray Method

G. Gnana kumar · B. Karunagaran · Kee Suk Nahm · R. Nimma Elizabeth

Received: 25 December 2008 / Accepted: 27 January 2009 / Published online: 18 February 2009

Abstract Spherical shaped, nanometer to micro meter sized silica particles were prepared in a homogeneous nature by spray technique. Silver nanoparticles were produced over the surface of the silica grains in a harmonized manner. The size of silver and silica particles was effectively controlled by the precursors and catalysts. The electrostatic repulsion among the silica spheres and the electro static attraction between silica spheres and silver particles make the synchronized structure of the synthesized particles and the morphological images are revealed by transmission electron microscope. The silver ions are reduced by sodium borohydride. Infra red spectroscopy and X-ray photoelectron spectroscopy analysis confirm the formation of silver–silica composite particles. Thermal stability of the prepared particles obtained from thermal analysis ensures its higher temperature applications. The resultant silver embedded silica particles can be easily suspended in diverse solvents and would be useful for variety of applications.

Keywords Attraction · Repulsion · Silver · Spray · Thermal

G. Gnana kumar · K. S. Nahm
Specialized Graduate School of Hydrogen and Fuel Cell Engineering, Chonbuk, National University, Jeonju 561-756, Republic of Korea

G. Gnana kumar
e-mail: gkumar_2006@yahoo.co.in

B. Karunagaran
Semiconductor Physics Research Center and Department of Semiconductor, Science and Technology, Chonbuk National University, Jeonju 561-756, Republic of Korea

K. S. Nahm (✉)
School of Chemical Engineering and Technology, Chonbuk National University, Jeonju 561-756, Republic of Korea
e-mail: nahmks@chonbuk.ac.kr

R. Nimma Elizabeth
Department of Physics, Lady Doak College, Madurai 625002, India

Introduction

The glory of nanomaterials is imperative and stimulated its various dimensions in nano-electronics, analytical chemistry, photonics, drug delivery, bio encapsulation, data recording media, gas sensing, storage, electronic, optical, and mechanical devices [1–7]. The large interfacial area, mechanical, chemical, and optical properties afforded by the nanomaterials promote the efficiency of the above fields. Besides, the effective characteristics such as quantum-size effect, nonlinear optical properties, and unusual luminescence than that of their bulk materials influence its viable applications [8–12]. But the applications of nanomaterials in industries have been hampered by the difficulty in controlling their size and morphology in a bulk amount. This impedes the commercial application of nanoparticles across the global industries than the micro particles. Various techniques have been adopted to synthesize the nanoparticles such as ultra sonication, pretreatment steps in electro less plating, electrostatic assemble method, and bi-functional composite method. The uncontrolled flow of chemicals by the above conventional methods leads to the aggregation as well as nonhomogeneous nature of the nanoparticles and even sometimes it leads to the formation of micro particles too. It has also degraded the product quality and could not provide the anticipated efforts in particle dispersal, which makes the application process tedious.

But through the spray technique, flow rate could be effectively controlled, which avoids the aggregation and promotes the homogeneous nature of the synthesized particles. The spray technique is well known for its rapidness, applicable for the heat-sensitive materials, simplicity, high purity, and the prospect of scale up [13, 14]. Among the nanoparticles, silica and silver have been extensively used in cosmetics, textiles, paints, bio-products, nanoscale electronic devices, photographic emulsions, catalysis, pigments, ceramics, optoelectronics, and the protection of environmentally sensitive materials [15–18]. The above-mentioned applications are being satisfied by a single material, i.e., either by silver or silica. By combining the above two materials, more remarkable properties can be achieved and influences its viable applications in various fields. In recent times, silver nanoparticles embedded silica particles have been of great interest due to their potential applications in electronic, optical, catalytic, bactericidal, and fungicidal fields [19–21]. Hence, an attempt was carried out for the synthesis of silver embedded silica particles by spray method. The structural characterization and thermal analysis of the synthesized particles are reported. Moreover, by simply changing the content of precursors and catalysts, a chance of nanometer to micrometer sized particles is guaranteed and has reported as follows.

Experimental Section

Tetra ethyl ortho silicate ($Si(OC_2H_5)_4$, TEOS), ammonium hydroxide (as a catalyst) distilled water, ethanol, silver nitrate, and sodium borohydride were used as source materials and were analytically pure. The spray equipment has been designed according to the procedure described previously [22]. Briefly, a quartz capillary nozzle is fitted with a reservoir. One end of the reservoir is connected with a round bottomed flask and another end is fixed with a pressure regulator for the flow of nitrogen. The synthesis of silica is described previously [13] and the synthesis of silver–silica composite particles is described as follows: appropriate amount of TEOS (7.5 wt% for 90 nm in ethanol solution, 20.38 wt% for 1 μm in ethanol solution) was taken in a reservoir. It was sprayed (pressure 10 psi) drop wise in to the mixture of ammonium hydroxide (4.25 wt% for 90 nm silica particles, 37.64 wt% for 1 μm silica particles in ethanol). Then appropriate amounts of aqueous silver nitrate solution (4.75 wt% for 6–9 nm silver particles, 9.20 wt% for 30–34 nm silver particles) and sodium borohydride were sprayed drop wise over the above mixture and continuously stirred for 4 h at room temperature. The particles were separated by the centrifugal machine. The separated particles were washed twice with ethanol by ultra sonication and dried in an oven at 80 °C for 4 h.

Conventional transmission electron microscope (TEM) micrographs were recorded on (JEOL JEM-2010). FT-IR spectra of the samples were recorded at room temperature using Jasco FT-IR-300 E in the region 400–4,000 cm^{-1}. Thermal gravimetric analysis was carried out using Perkin Elmer instrument. The TGA measurements were carried out under a nitrogen atmosphere with a heating rate of 10 °C/min from 30 to 800 °C. X-ray photoelectron spectroscopy (XPS) analysis was carried out on a Kratos Amicus spectrometer (Kratos Analytical Ltd. Manchester, England). The PL spectra of the synthesized particles were measured by a spectrometer with a CCD detector (Jasco, FP-6500).

Results and Discussion

Figure 1 shows the TEM microscopic images of silica particles. From the images, it is clear that mono dispersed and smooth surfaced 90-nm silica particles were obtained from spray method under base-catalyzed condition. Figure 2 a, b reveals the silver embedded nanometer sized silica particles. The silver nanoparticles in the range of 3 to 6 nm were homogeneously mobilized over the surface of the silica particle. The incorporation of silver particles does not change the spherical morphology of silica particles. Figure 2c indicates a much closer view of the silver

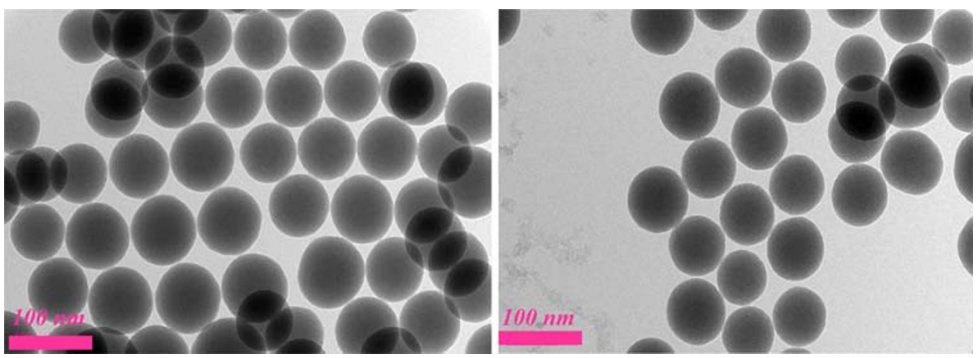

Fig. 1 TEM images of 90 nm silica particles

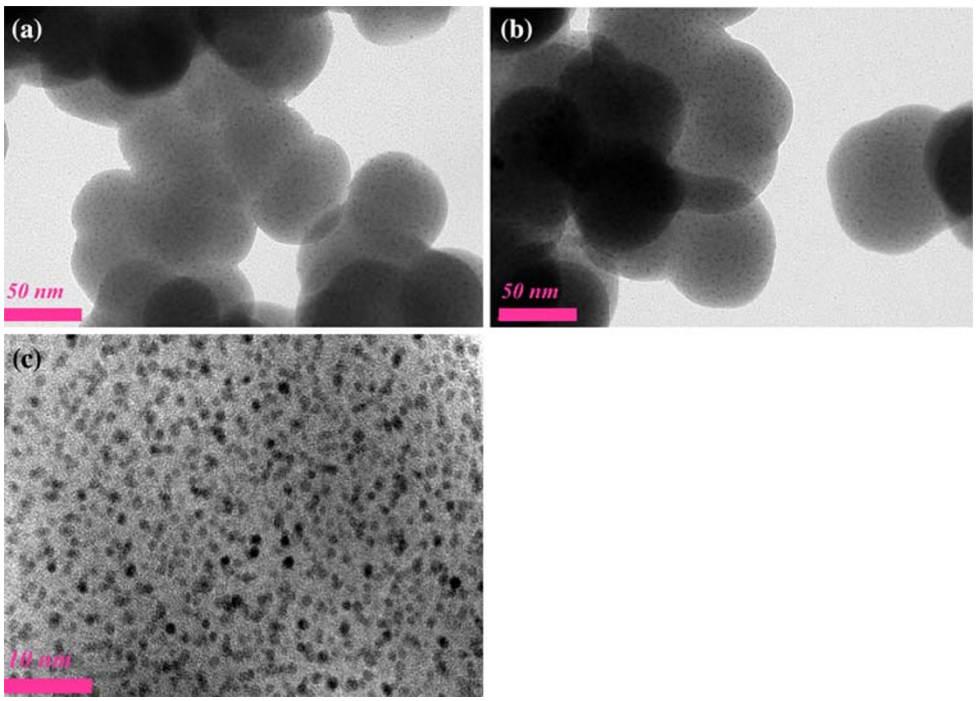

Fig. 2 TEM images of **a**, **b** 3–6 nm sized silver embedded 90 nm silica particles and **c** a closer view of the silver nanoparticles

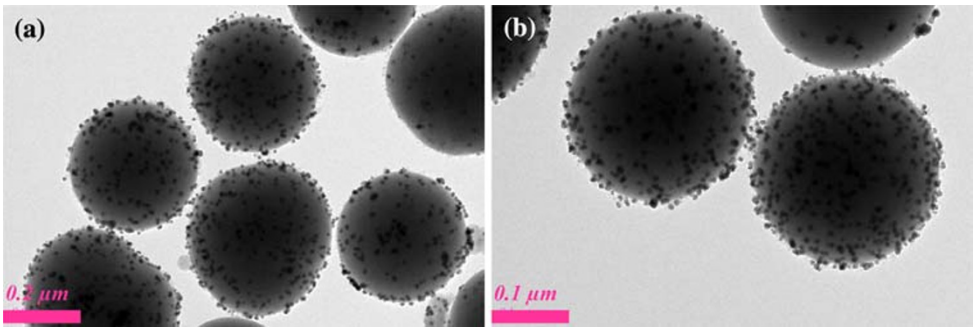

Fig. 3 TEM images of **a**, **b** 30–34 nm sized silver embedded 1 μm silica particles

particles embedded on the silica particle and ensures the homogeneous nature of the synthesized silver nanoparticles. The hydrolysis of tetra ethyl ortho-silicate (TEOS) under alkaline condition resulted the $Si(OH)_4$ tetrahedra. It is followed by the condensation (polymerization) of the dispersed phase material, which yielded three dimensional silica nanospheres. The inclusion of ammonia promotes the hydrolysis, which facilitated the condensation rate and results in faster kinetics. The formed spherical shaped silica particles are negatively charged under alkaline condition and the repulsive electric forces highly capitulate mono dispersed silica spheres [23]. The added aqueous $AgNO_3$ solution has reduced in to silver ions by the inclusion of sodium borohydride ($NaBH_4$). The reduced silver particles possess the positive charge and are being adsorbed on the surface of the silica particles, which were negatively charged. The silver ions were reduced first and then have become the nucleus for the deposition of the nanosilver on the silica particles. The electro static repulsion experienced between the silica nanospheres avoid the aggregation, whereas the electro static attraction between the silica spheres and silver leads to the attachment of Ag particles on the silica surface. Figure 3 reveals the 30–34 nm sized silver particles embedded on the 1 μm sized silica particles. From this, it is clear that with the variation of silica and silver precursors concentration, nanometer to micrometer ranged homogeneous particles could be prepared without the change in any experimental parameters. An increase in the precursors concentration effectively promotes the size of the synthesized particles. The enrollment of controlling size and homogeneity of the silver embedded silica particles by the conventional methods is tedious but from the spray technique nanometer to micrometer sized particles can be effectively controlled and ensures its viable applications in various fields. Figure 4 reveals the EDX spectrum, and the presence of Si, Ag, and oxygen elements indicates the formation of the pure silver–silica composite.

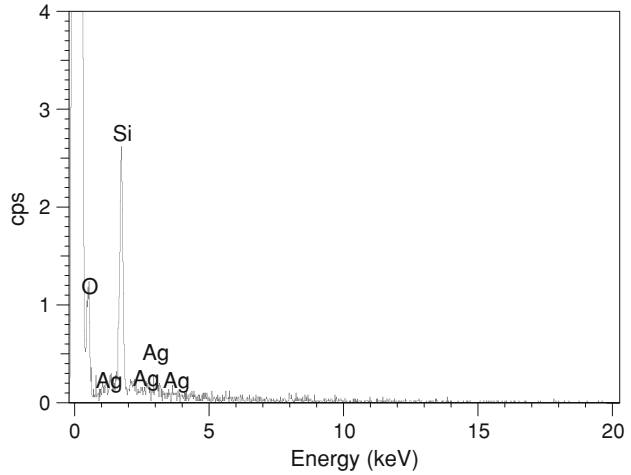

Fig. 4 EDX spectrum of silver embedded silica particles

Figure 5 shows the IR profile of pure silica and silver embedded silica particles, the characteristic bands were assigned as follows: the broad characteristic bands observed at 3,440 and 1,640 cm^{-1} are attributed for the O–H stretching of molecular adsorbed water with hydrogen bonds or to isolate OH and to the H–O–H bending vibration of molecular water, respectively. The asymmetric LO and TO stretching bonds ≡Si–O–Si≡ of the SiO_4 tetrahedron were assigned for the peaks found at 1,106 cm^{-1} along with the accompanied shoulder at 1,398 cm^{-1}, respectively. The shoulder found at 953 cm^{-1} attributed to the Si–O–H stretching vibrations. Si–O–Si symmetric stretch of the obtained silica particles was observed at 800 cm^{-1}. Si –O–Si or O–Si– O bending mode was observed at sharp one located at 469 cm^{-1} and was shifted to 471 cm^{-1} for silica–silver composite. An intense peak found at 1,384 cm^{-1} was attributed for the silver particles (Fig. 5b) [13, 24]. The separate bands for the silver–silica composites have not found out with a high intensity and narrow width for the synthesized samples. But all the characteristic bands of silica were shifted for the silver embedded silica particles. The split and shifts of bands observed from the IR spectra indicate the formation of silver embedded silica matrix [25]. Since only infrared peaks related to the SiO_2 surface layer and silver observed from the infra red spectroscopic analysis indicates the high purity of the prepared sample.

The thermal analysis of the prepared samples is given in Fig. 6. A low percentile weight loss was observed for the synthesized silica and silver embedded silica particles. The first main weight loss was observed at around 100 °C and attributed for the evaporation of weakly adsorbed water molecules. The weight losses observed for silica and silver embedded silica were 7.1% and 3.4%, respectively for this region. The condensation of silanol groups yielded the second weight loss at 200–350 °C. Here, the thermal weight loss of silica and silver embedded silica were 8.32% and 8.49%, respectively. The loss of water molecule via condensation of silanol groups resulted in the third weight loss at 700–800 °C and the thermal weight losses observed in this stage were 10.85% and 12.62% [13, 26]. At lower temperatures, pure silica particle experiences lower thermal stability than the silver–silica composite material. Though the incorporation of silver nanoparticles over the silica matrix experiences lower thermal stability at higher temperatures, a lower weight percentile loss obtained from the thermal analysis ensures the thermal stability of the synthesized silver embedded silica particles.

Figure 7 reveals the XPS spectrum of pure silica and silver–silica composite matrix. The strong peaks observed at 101.75 and 152 eV reveal the Si_{2P} and Si_{2S} spectrum and confirm the presence of silica (Fig. 7a) [27]. The peak found at 531.84 eV shows the O_{1S} spectrum and attributed

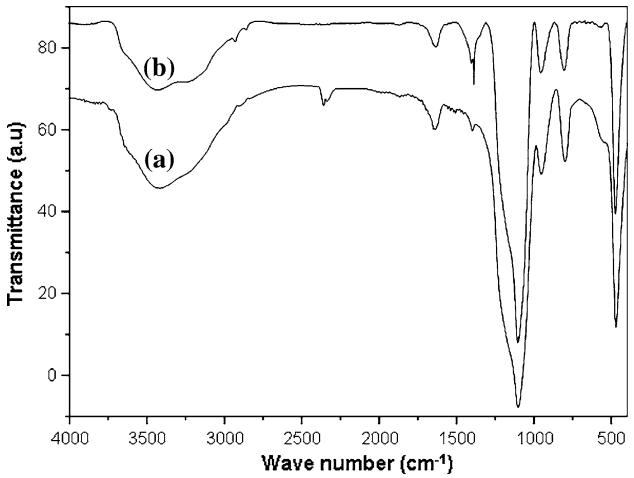

Fig. 5 IR profile of (a) silica particles and (b) silver embedded silica particles

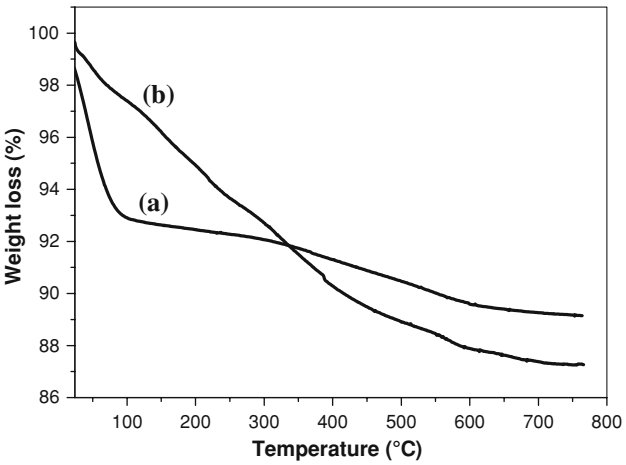

Fig. 6 Thermal analysis: (a) silica particles and (b) silver embedded silica particles

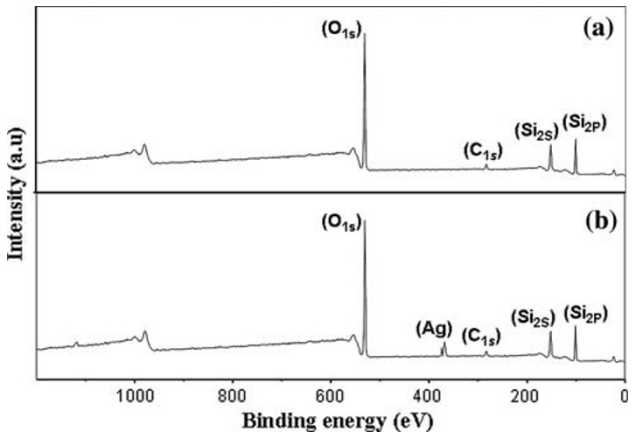

Fig. 7 XPS spectrum of (a) silica particles and (b) silver embedded silica particles

to the OH groups, which are present in the surface of silica [28]. Besides, a weak C_{1S} peak was also observed at 282.4 eV in pure silica sample (Fig. 7a). This C_{1S} signal might be due to the incomplete hydrolysis of the alkoxide precursor used for the synthesis of the pure silica particles. These peaks confirm the formation of silica particle. The above-mentioned pure silica XPS peaks were also observed for the silver embedded silica particles as shown in Fig. 7b. Besides, a doublet band observed at about 368.8 and 374.6 eV corresponds to the $Ag3d_{5/2}$ and $Ag3d_{3/2}$ spectrums, respectively, and confirms the presence of silver over the surface of the silica particles [29]. No other peaks observed in the XPS spectrum confirm the high purity of the prepared samples.

Figure 8 reveals the PL spectrum of pure silica and silver–silica composites under the excitation wavelength of 250 nm. For the pure silica particles, a strong peak observed at 301 nm was attributed for the origination of two-fold-coordinated silicon lone-pair centers (≡O–Si–O≡). It corresponded to the intrinsic diamagnetic defect centers. For bare silica, both the photo excitation and radiative recombination occurred within itself, whereas for silver-loaded silica the distinguished increase in PL intensity was observed. The PL emission at 310–370 nm from porous silicon prepared by high temperature oxidation [30] or from the silicon oxide film prepared with various deposition techniques [31] has been observed and attributed to the oxygen excess defects, such as a peroxy linkage –Si–O–O–Si–. Qin et al. [32] have reported that the SiO_2 powder annealed in O_2 at high temperature has a PL peak at 370 nm and an obvious PLE peak at 280 nm monitored at the emission wavelength. Garcia et al. [33] have found that the silica coatings prepared via sol–gel in air show a PL spectrum dominated by a peak at 370 nm upon excitation with 322 nm light. In this study, the PL peak observed at 310 nm is associated with the ≡Si–Si≡ oxygen vacancies. During the implantation of silver ions over a silica matrix, a large extent of structural defects were resulted from the splitting of the perfect ≡Si–O–Si≡ network and a peak at 310 nm ensures the large concentration of ≡Si—Si≡ oxygen vacancies. This oxygen vacancy is created by electronic excitation effect as well as chemical reaction. Electronic excitation creates depth profile of Si–Si bonds, whereas chemical reaction creates the profile of implanted silver ions. When the chemical reaction is predominant, implanted ions chemically react with oxygen atoms in the silica network structure for the formation of implant-oxygen bonds and leaving Si–Si bonds [34]. The PL peak found at 358 nm was attributed to the atomic silver. The Ag oligomers dispersed within the pores of silica formed by the reduction of $AgNO_3$ were clearly evidenced from the above peak and ensure their complete incorporation and higher chemical stability [35]. The harmonious distribution of nanosized silver particles, optical, electrical, catalytic, microbicidal properties of the composite makes its potential application in nano-electronics, nonlinear optical devices, catalysts, delivery of drugs, sensors, bactericidal, and fungicidal fields and are assigned as follows: silver–silica composite

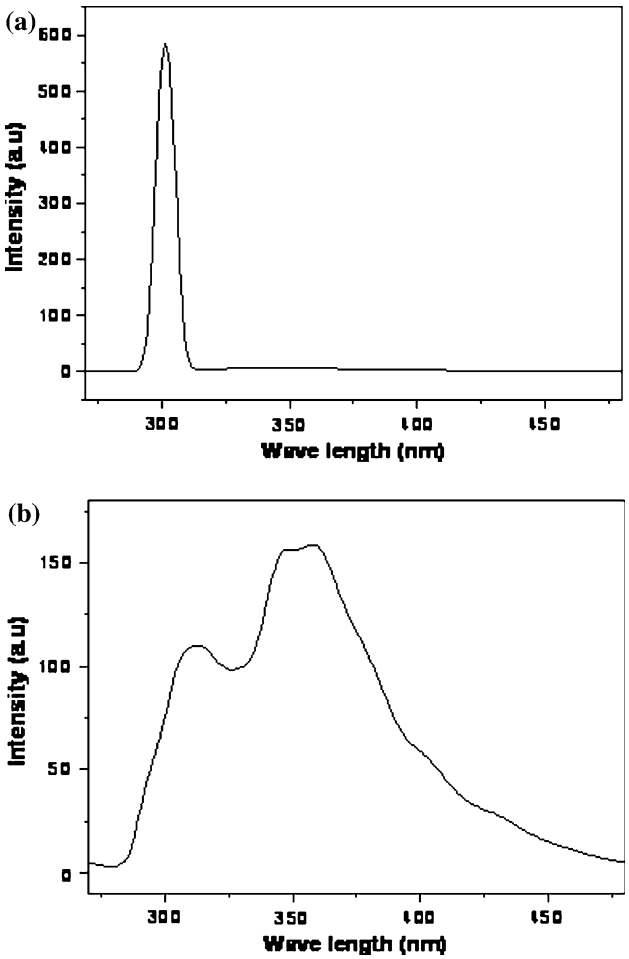

Fig. 8 PL spectrum of **a** silica particles and **b** silver embedded silica particles

materials exhibit excellent antibacterial characteristics even at the lower concentrations and are nontoxic. Organic materials based antibacterial agents are chemically unstable and cannot be utilized under precise conditions. But it was effectively tackled by the silver embedded silica particles due to its high anti antibacterial and chemical durability. In general, the oxidation of alcohols had been catalyzed by chromium. Due to its high cost and harmful nature, it was greatly avoided for utilization. The silver–silica composite catalyst induces the high conversion rate of the alcohols oxidation due to its highly exposed surface, which is responsible for more reaction sites [36]. The presence of silver clusters in silica promotes the third-order optical non-linear susceptibility, which leads to an intensity-dependent refractive index thus allowing the scheduling and the development of all-optical switching devices. The well-adsorbed silver nanoparticles inside the channel of silica completely reduce the catalyst leaking. It makes the catalyst stable and anti-contaminated, which lead to a promoted sensor for the determination of hydrogen peroxide [37]. The tunable pore sizes with narrow distributions and well-defined surface properties of the composite allowing them to adsorb certain kinds of drugs and release these drugs in a more reproducible manner and find their application in drug delivery [38]. Besides the present results suggest that the fused silica could generate different photoluminescence emission, excited with different incident beams, which can be interesting for applications in the optoelectronic field.

Conclusion

With the variation of precursors and ammonium hydroxide, silver embedded silica particles with different particle sizes were synthesized. Harmonized size and spherical shape of the particles were confirmed by morphological images. EDX, infra red spectroscopy, and XPS measurements ensure the formation of silver embedded silica particles and its high purity. Harmonized distribution of silver embedded silica particles prepared by the novel spray technique has proven as a prevailing approach for the synthesis of silver embedded silica nanoparticles.

Acknowledgment This work was supported by the Ministry of Knowledge Economy (MKE) through the Specialized Graduate School program. The authors convey their heart felt gratitude to Dr. Senthilarasu, Chonbuk National University, Republic of Korea for his guidance.

References

1. Y. Tabata, Protein Nanotechnol. **300**, 81 (2008). doi:10.1385/1-59259-858-7:081
2. R.D. Handy, R. Owen, E.V. Jones, Ecotoxicology **17**, 315 (2008). doi:10.1007/s10646-008-0206-0
3. W.Y. Li, L.N. Xu, J. Chen, Adv. Funct. Mater. **15**(5), 851 (2005). doi:10.1002/adfm.200400429
4. J. Zygmunt, F. Krumeich, R. Nesper, Adv. Mater. **15**, 1538 (2003). doi:10.1002/adma.200305134
5. N.I. Kovtyukhova, T.E. Mallouk, T.S. Mayer, Adv. Mater. **15**, 780 (2003). doi:10.1002/adma.200304701
6. J. Jang, H. Yoon, Adv. Mater. **16**, 799 (2004). doi:10.1002/adma.200306567
7. R.V. Ramanujan, Sadhana **8**(1–2), 81 (2003). doi:10.1007/BF02717127
8. G.R. Patzke, F. Krumeich, R. Nesper, Angew. Chem. Int. Ed. **41**, 2446 (2002). doi:10.1002/1521-3773(20020715)41:14<2446::AID-ANIE2446>3.0.CO;2-K
9. R. Tenne, Angew. Chem. Int. Ed. **42**, 5124 (2003). doi:10.1002/anie.200301651
10. L. Miao, S. Tanemura, S. Toh, K. Kaneko, M. Tanemura, J. Cryst. Growth **264**(1–3), 246 (2004). doi:10.1016/j.jcrysgro.2003.12.027
11. T. Abe, Y. Tachibana, T. Uematsu, M. Iwamoto, J. Chem. Soc. Chem. Commun. **16**, 1617 (1995). doi:10.1039/c39950001617
12. A.D. Yoffe, Adv. Phys. **42**(2), 173 (1993). doi:10.1080/00018739300101484
13. G. Gnanakumar, S. Senthilarasu, D.N. Lee, A.R. Kim, P. Kim, K.S. Nahm, S.H. Lee, R.N. Elizabeth, Synth. Met. **158**, 684 (2008). doi:10.1016/j.synthmet.2008.04.031
14. T. Dedova, O. Volobujeva, J. Klauson, A. Mere, M. Krunks, Nanoscale Res. Lett. **2**, 391 (2007). doi:10.1007/s11671-007-9072-6
15. B. Khlebtsov, L. Dykman, V. Bogatyrev, V. Zharov, N. Khlebtsov, Nanoscale Res. Lett. **2**, 6 (2007). doi:10.1007/s11671-006-9021-9
16. C. Ren, J. Li, Q. Liu, J. Ren, X. Chen, Z. Hu, D. Xue, Nanoscale Res. Lett. **3**, 496 (2008). doi:10.1007/s11671-008-9186-5
17. H.L. Pape, F.S. Serena, P. Contini, C. Devillers, A. Maftah, P. Leprat, Carbon **40**(15), 2947 (2002). doi:10.1016/S0008-6223(02)00246-4
18. S. Angloher, J. Kecht, T. Bein, Microporous Mesoporous Mater. **115**(3), 629 (2008). doi:10.1016/j.micromeso.2008.02.019
19. M. Kawashita, S. Toda, H.M. Kim, T. Kokubo, N. Masuda, J. Biomed. Mater. Res. A **66A**(2), 266 (2003). doi:10.1002/jbm.a.10547
20. S.D. Oh, S. Lee, S.H. Choi, I.S. Lee, Y.M. Lee, J.H. Chun, H. Park, J. Colloid Surf. A Physicochem. Eng. Asp. **275**, 228 (2006)
21. M. Jasiorski, S. Bakardijeva, W. Doroszkiewicz, S. Brzezinski, G. Malinowska, D. Marcinkowska, M. Ornat, W. Strek, K. Maruszewski, Mater. Sci. **22**(2), 137 (2004)
22. A.G. Howard, N.H. Khdary, Mater. Lett. **61**, 1951 (2007). doi:10.1016/j.matlet.2006.07.110
23. W. Stober, A. Fink, J. Colloid Interface Sci. **26**, 62 (1968). doi:10.1016/0021-9797(68)90272-5
24. L. Li, G. Li, R.L.J. Smith, H. Inomata, Chem. Mater. **12**, 3705 (2000). doi:10.1021/cm0004811
25. J.A. Banos et al., J. Sol-Gel Sci. Technol. **30**, 89 (2004). doi:10.1023/B:JSST.0000034696.92285.72
26. S.S. Choi, S.G. Lee, S.S. Im, S.H. Kim, Y.L. Joo, J. Mater. Sci. Lett. **22**, 891 (2003). doi:10.1023/A:1024475022937
27. C. Carriere, D. Brion, J. Escard, J.P. Deville, J. Electron Spectrosc. Rel. Phenom. **10**, 85 (1977). doi:10.1016/0368-2048(77)85006-8
28. A.S. Lim, A. Atrens, Appl. Phys. A **51**, 411 (1990). doi:10.1007/BF00348382
29. L. Jiang, W. Wang, D. Wu, J. Zhan, Q. Wang, Z. Wu, R. Jin, Mater. Chem. Phys. **104**, 230 (2007). doi:10.1016/j.matchemphys.2007.03.023

30. J. Lin, G.Q. Yao, J.Q. Duan, G.G. Qin, Solid State Commun. **97**, 221 (1996). doi:10.1016/0038-1098(95)00650-8
31. T. Kanashima, M. Okuyama, Y. Hamakawa, Appl. Surf. Sci. **79–80**, 321 (1994). doi:10.1016/0169-4332(94)90430-8
32. G.G. Qin, J. Lin, J.Q. Duan, G.Q. Yao, Appl. Phys. Lett. **69**, 1689 (1996). doi:10.1063/1.117029
33. M.A. García, S.E. Paje, M.A. Villegas, J. Llopis, Mater. Lett. **43**, 23 (2000). doi:10.1016/S0167-577X(99)00224-4
34. G. De, A. Licciulli, C. Massaro, L. Tapfer, M. Catalano, G. Battaglin, C. Meneghini, P. Mazzoldi, J. Non-Cryst. Solids **194**, 225 (1996)
35. G.M. Castanon, J.R. Martinez, G.O. Zarzosa, F. Ruiz, J. Sol-Gel Sci. Technol. **36**, 137 (2005)
36. E.V. Kondratenko, M. Cherian, M. Baerns, D. Su, R. Schlögl, X. Wang, I.E. Wachs, J. Catal. **234**, 131 (2005)
37. D.H. Lin, Y.X. Jiang, Y. Wang, S.G. Sun, J. Nanomater. **10**, 1 (2008)
38. N. Sounderya, Y. Zhang, Recent Pat. Biomed. Eng. **1**, 34 (2008)